Implicit 3-D depth migration by wavefield extrapolation with helical boundary conditions

James Rickett, Jon Claerbout and Sergey Fomel, Stanford University

SUMMARY

Wavefield extrapolation in the $(\omega - x)$ domain provides a tool for depth migration with strong lateral variations in velocity. Implicit formulations of depth extrapolation have several advantages over explicit methods. However, the simple 3-D extension of conventional 2-D wavefield extrapolation by implicit finite-differencing requires the inversion of a 2-D convolution matrix which is computationally difficult. In this paper, we solve the $45°$ wave equation with helical boundary conditions on one of the spatial axes. These boundary conditions reduce the 2-D convolution into an equivalent 1-D filter operation. We then factor this 1-D filter into causal and anti-causal parts using an extension of Kolmogoroff's spectral factorization method, and invert the convolution operator efficiently by 1-D recursive filtering. We include lateral variations in velocity by factoring spatially variable filters, and non-stationary deconvolution. The helical boundary conditions allow the 2-D convolution matrix to be inverted directly without the need for splitting approximations, with a cost that scales linearly with the size of the model space. Using this methodology, a whole range of implicit depth migrations may now be feasible in 3-D.

INTRODUCTION

Implicit 2-D finite-difference wavefield extrapolation has proved itself as a robust, accurate migration method (Claerbout, 1985). It naturally and efficiently deals with lateral variations in velocity without the need for asymtotic approximations, such as ray-tracing. The implicit formulation also ensures unconditional stability. Unfortunately, despite the exponential growth of 3-D seismology, implicit 3-D wavefield extrapolation has yet to find wide-spread application. Whereas 2-D extrapolation requires the inversion of a tridiagonal system, the simple extension from 2-D to 3-D leads to a blocked tridiagonal system, which is prohibitively expensive to solve.

Typically, the matrix inversion problem is avoided by an explicit finite-difference approach (Holberg, 1988). Explicit extrapolation has proved itself effective for pratical 3-D problems; since stable explicit filters can be designed (Hale, 1990b), and McClellan filters provide an efficient implementation (Hale, 1990a). However, unlike implicit methods, stability can never be guaranteed if there are lateral variations in velocity (Etgen, 1994). Additionally, accuracy at steep dips requires long explicit filters, which cannot handle rapid lateral velocity variations, and can be expensive to apply.

The problem can also be avoided by splitting the operator to act sequentially along the x and y axes. Unfortunately this leads to azimuthal operator anisotropy, and requires an additional phase correction operator (Graves and Clayton, 1990). Zhou and McMechan (1997) have presented an alternative to the traditional $45°$ equation, with form similar to the $15°$ equation plus an additional correction term. Although splitting their equations results in less azimuthal anisotropy than with the standard $45°$ equation, the splitting approximation is still needed to solve the equations.

We apply helical boundary conditions (Claerbout, 1998), to simplify the structure of the matrix, reducing the 2-D convolution to an equivalent problem in one dimension. The 1-D convolution matrix can be factored into a pair of causal and anti-causal filters, thereby providing an LU decomposition. The factorization is based on Kolmogoroff's spectral method, but with an extension to handle cross-spectra. The filters are then inverted efficiently by recursive polynomial division. We also allow for laterally variable velocity by factoring spatially varying filters, followed by non-stationary deconvolution.

Very accurate implicit methods have been developed for 2-D migrations (e.g. Jenner et al., 1997) without obvious extensibility to 3-D.

Although we only solve the $45°$ wave equation in this paper, the helical boundary conditions provide a practical way to apply implicit migrations of higher accuracy in 3-D.

IMPLICIT EXTRAPOLATION

The basis for wavefield extrapolation is an operator, $W(k)$, that marches the wavefield P, at depth z, down to depth $z + 1$.

$$P_{z+1} = W(k)\, P_z \tag{1}$$

Ideally, $W(k)$, will have the form of the phase-shift operator (Gazdag, 1978).

$$W(k) = e^{i\sqrt{a^2 - k^2}} \tag{2}$$

where $a = \omega/v$, and for simplicity $\Delta x = \Delta z = 1$.

However, to apply this operator directly requires spatial Fourier transforms, and an assumption of constant lateral velocity. To overcome this limitation, short finite-difference approximations to $W(k)$ are applied in the $(\omega - x)$ domain.

An implicit finite-difference formulation approximates $W(k)$ with a convolution followed by an inverse convolution. For example, a simple implicit approximation to equation (1) that corresponds to the Crank-Nicolson scheme for the $45°$ one-way wave equation, is given by

$$W_{im}(k) = e^{ia}\,\frac{1 - 4a^2 + iak^2}{1 - 4a^2 - iak^2} = e^{i\phi} \tag{3}$$

where $\phi = a - \arctan\frac{ak^2}{4a^2 - 1}$. Since this operator represents a phase-shift only, energy is conserved, and the formulation is unconditionally stable for all values of a.

An explicit approach approximates $W(k)$ directly with a single convolutional filter. For example, a three-term expansion of equation (1) yields

$$W_{ex}(k) = e^{ia}\,\left(1 + \gamma_1 k^2 + \gamma_2 k^4\right) \tag{4}$$

where complex coefficients γ_1 and γ_2 can be calculated using some kind of Taylor series, for example.

Although in practice stability is not usually a problem for explicit operators, they can never represent a pure phase-shift. Hence, stability cannot be guaranteed for all velocitiy models.

Also in order to preserve high angular accuracy for steep dips, explicit filters need to be longer than their implicit counterparts. The advantage of finite-difference methods over Fourier methods is that the effect of the finite-difference convolution filters is localized, leading to accurate results for rapidly varying velocity models. This is less of an advantage for long filters.

The $45°$ wave equation

The diffraction term of the in the $45°$ equation (Claerbout, 1985) can be rewritten as the following matrix equation, by inserting the rational part of the implicit extrapolator (3) into equation (1):

$$(\mathbf{I} + \alpha_1 \mathbf{D})\,\mathbf{q}_{z+1} = (\mathbf{I} + \alpha_2 \mathbf{D})\,\mathbf{q}_z \tag{5}$$

$$\mathbf{A}_1 \mathbf{q}_{z+1} = \mathbf{A}_2 \mathbf{q}_z \tag{6}$$

where the complex coefficients α_1 and α_2 can be calculated, and $\mathbf{D}$ is a finite-difference representation of the Laplacian, ∇^2.

3D wavefield extrapolation with helical boundary conditions

The right-hand-side of equation (6) is known. The challenge is to find the vector $\mathbf{q}_{z+1}$ by inverting the matrix, $\mathbf{A}_1$. Given the wavefield on the surface, this equation provides a way to downward-continue in depth.

The matrices in equation (6) represent convolution with a scaled finite-difference Laplacian, with its main diagonal stabilized. Scaling coefficients, α_1 and α_2, are complex and depend on the ratio, ω/v.

In the two-dimensional problem, the ∇^2 operator acts only in the x-direction, and can be represented by the three-point convolutional filter, $d = (1, -2, 1)$. The matrix, $\mathbf{A}_1$, therefore, has a tridiagonal stucture, which can be inverted efficiently with a recursive solver.

In three-dimensional wavefield extrapolation, the ∇^2 operator acts in both the x and y-directions. $\mathbf{A}_1$ and $\mathbf{A}_2$ therefore represent 2-D convolution, and d can be represented by the a simple 5-point filter,

$$d = \begin{bmatrix} & 1 & \\ 1 & -4 & 1 \\ & 1 & \end{bmatrix} \tag{7}$$

or a more isotropic 9-point filter (Iserles, 1996),

$$d = \begin{bmatrix} 1/6 & 2/3 & 1/6 \\ 2/3 & -10/3 & 2/3 \\ 1/6 & 2/3 & 1/6 \end{bmatrix} \tag{8}$$

The vectors $\mathbf{q}_z$ and $\mathbf{q}_{z+1}$ contain the wavefield at every point in the (x,y)-plane. Therefore, the convolution matrices that operate on them are square with dimensions $N_x N_y \times N_x N_y$. As an illustration, for a 4×2 spatial plane, the structure of matrix $\mathbf{D}$ with the five-point approximation and transient boundary conditions, will be the blocked-tridiagonal matrix

$$\mathbf{D} = \left[\begin{array}{cccc|cccc} -4 & 1 & . & . & 1 & . & . & . \\ 1 & -4 & 1 & . & . & 1 & . & . \\ . & 1 & -4 & 1 & . & . & 1 & . \\ . & . & 1 & -4 & . & . & . & 1 \\ \hline 1 & . & . & . & -4 & 1 & . & . \\ . & 1 & . & . & 1 & -4 & 1 & . \\ . & . & 1 & . & . & 1 & -4 & 1 \\ . & . & . & 1 & . & . & 1 & -4 \end{array} \right] \tag{9}$$

This pentadiagonal system cannot be easily inverted, even for the case of constant velocity, since the missing coefficients on the second diagonals break the Toeplitz structure.

HELICAL BOUNDARY CONDITIONS

The helix transform (Claerbout, 1998) provides boundary conditions that map multi-dimensional convolution into one-dimension. In this case, the 2-D convolution operator, $(\alpha_1 \mathbf{I} + \mathbf{D})$, can be recast as an equivalent 1-D filter.

Helical boundary conditions allow the two-dimensional convolution matrix, $\mathbf{A}_1$, to be expressed as a one-dimensional convolution with a filter of length $2N_x + 1$ that has the form

$$a_1 = (1, 0, \ldots 0, 1, \alpha_1 - 4, 1, 0, \ldots 0, 1)$$

The structure of the finite-difference Laplacian operator, $\mathbf{D}$, is simplified when compared to equation (9).

$$\mathbf{D} = \begin{bmatrix} -4 & 1 & . & . & 1 & . & . & . \\ 1 & -4 & 1 & . & . & 1 & . & . \\ . & 1 & -4 & 1 & . & . & 1 & . \\ . & . & 1 & -4 & 1 & . & . & 1 \\ 1 & . & . & 1 & -4 & 1 & . & . \\ . & 1 & . & . & 1 & -4 & 1 & . \\ . & . & 1 & . & . & 1 & -4 & 1 \\ . & . & . & 1 & . & . & 1 & -4 \end{bmatrix} \tag{10}$$

The 1-D filter can be factored into a causal and anti-causal parts, and the matrix inverse can be computed by recusive polynomial division (1-D deconvolution).

Cross-spectral factorization

Kolmogoroff spectral factorization (Claerbout, 1976) provides an alogorithm for finding a minimum-phase wavelet with a desired spectrum, or auto-correlation function.

Since positive-definite Hermitian matrices with Toeplitz structure represent convolutions with auto-correlation functions, Kolmogoroff provides a way to efficiently decompose them into the product of lower (causal) and upper (anti-causal) parts. Once this LU factorization has been achieved, the two parts can be inverted rapidly by recursion (polynomial division).

Unfortunately, the complex scale-factor, α_1, means $\mathbf{A}_1$ is symmetric, but not Hermitian, so the standard Kolmogoroff factorization will fail. Fortunately, however, the method can be extended to factor any cross-spectrum into a pair of minimum phase wavelets and a delay. The algorithm follows the standard Kolmogoroff factorization; however, negative lags are kept separately rather than being discarded.

The Kolmogoroff factorization is not exact because the filters are factored in the frequency domain, assuming circular boundary conditions; while the polynomial division is performed in the time domain with transient boundary conditions. As a result the filters must be padded in the time-domain before spectral factorization. Padding does not effect the overall cost of the migration, as the computational expense lies in the polynomial division, not in the factorization.

Alternative methods for cross-spectral factorization may avoid the circular boundary condition problem. For example, Wilson (1969) provides an algorithm based on Newton's recursive linearization that can efficiently factor polynomials (J. P. Burg, personal communication), and we have developed its extension to cross-spectra.

Polynomial division

Kolmogoroff cross-spectral factorization, therefore, provides a tool to factor the helical 1-D filter of length $2N_x + 1$ into minimum-phase causal and anti-causal filters of length N_x. Fortunately, filter coefficients drop away rapidly from either end. In practice, small-valued coefficients can be safely discarded, without violating the minimum-phase requirement; so for a given grid-size, the cost of the matrix inversion scales linearly with the size of the grid.

The unitary form of equation (3) can be maintained by factoring the right-hand-side matrix, $\mathbf{A}_2$ in equation (6), with Kolmogoroff before applying it to $\mathbf{q}_z$.

$$\mathbf{L}_1 \mathbf{U}_1 \, \mathbf{q}_{z+1} \quad = \quad \mathbf{L}_2 \mathbf{U}_2 \, \mathbf{q}_z \tag{11}$$
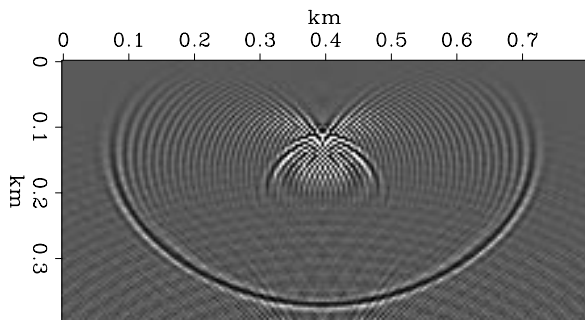
3D wavefield extrapolation with helical boundary conditions

Figure 1: Vertical slice through broad-band impulse response of 45°
wave equation, showing the distinctive cardioid.

$$\mathbf{q}_{z+1} \quad = \quad \frac{\mathbf{L}_2 \mathbf{U}_2}{\mathbf{L}_1 \mathbf{U}_1} \mathbf{q}_z \tag{12}$$

Impulse response

A slice through the broad-band impulse response of the 45° equation
is shown in Figure 1. As with the 2-D implementation of the 45°
equation, evanescent energy at high dip appears as noise, and takes the
form a cardioid. This is never a problem on field data, and has been
removed from the depth-slice shown in Figure 2. Implicit migration
with the full Laplacian, instead of a splitting approximation, produces
an impulse response that is azimuthally isotropic without the need for
any phase corrections.

Figure 3 shows the effects of the different boundary conditions on the
two spatial axes. The fast spatial axis (top and bottom of figure) have
helical boundary conditions, and show wrap-around. The slow spatial
axis (left and right of figure) has a zero-value boundary condition, and
hence is reflective.

For the examples in this paper, we set the 'one-sixth' parameter (Claer-
bout, 1985), $\beta_{1/6} = 0.125$, and used the isotropic nine-point Lapla-
cian from equation (8).

LATERAL VELOCITY VARIATIONS

While we have only described the factorization for $v(z)$ velocity mod-
els, the method can also be extended to handle lateral variations in
velocity.

For every value of ω/v, we precompute the factors of the 1-D heli-
cal filters, a_1 and a_2. Filter coefficients are stored in a look-up table.
We then extrapolate the wavefield by non-stationary convolution, fol-
lowed by non-stationary polynomial division. The convolution is with
the spatially variable filter pair corresponding to a_2. The polynomial
division is with the filter pair corresponding to a_1. The non-stationary
polynomial division is exactly analogous to time-varying deconvolu-
tion, since the helical boundary conditions have converted the two-
dimensional system to one-dimension.

Since we interpolate filters, not migrated wavefields as in 'split-step'
migration (Stoffa et al., 1990), the number of reference velocities used
has minimal effect on the overall cost of the migration.

Synthetic example

Figure 4 shows 2-D cross-sections through the simple 3-D synthetic
model used to test lateral velocity variations. The velocity model con-
sisted of a linear gradient of $0.85s^{-1}$ dipping at 45°. The reflec-
tivity model consisted of three 'bench'-shaped reflectors with dips of
15°, 35° and 50°. The synthetic data were modeled with a Kirchhoff
method, and a dip-limited impulse was added to the zero-offset section
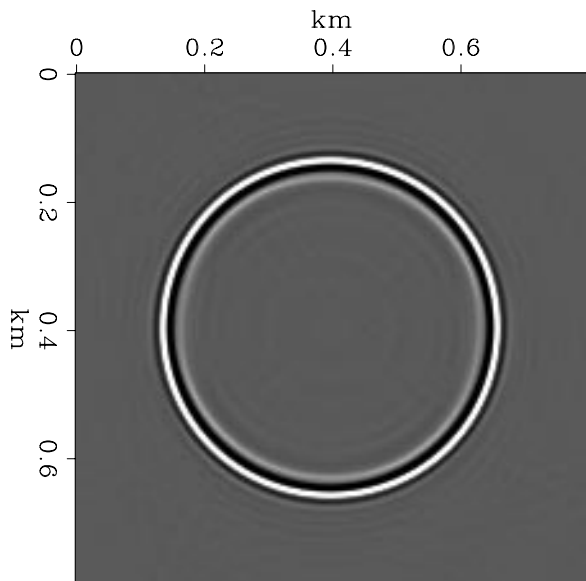to illustrate the 3-D nature of the algorithm.

Figure 2: Depth-slice of centered impulse response corresponding to
a dip of 45°. Note the azimuthally isotropic nature of the full implicit
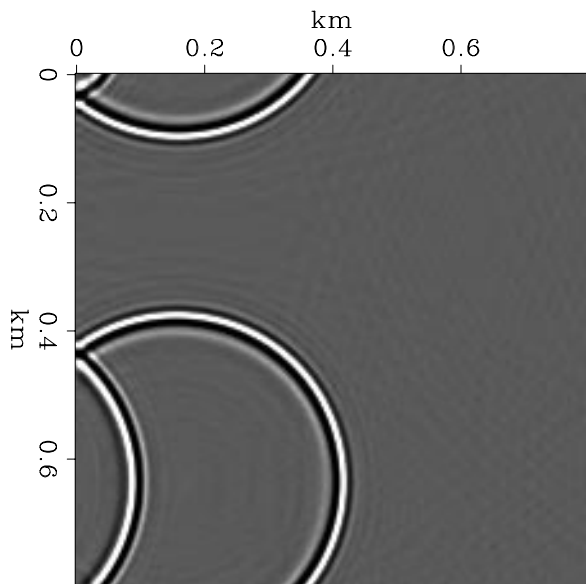migration. Evanescent energy has been removed by dip-filtering prior
to migration.

Figure 3: Depth-slice of offset impulse response corresponding to a
dip of 45°. Note the helical boundary conditions on the fast spatial
axis.

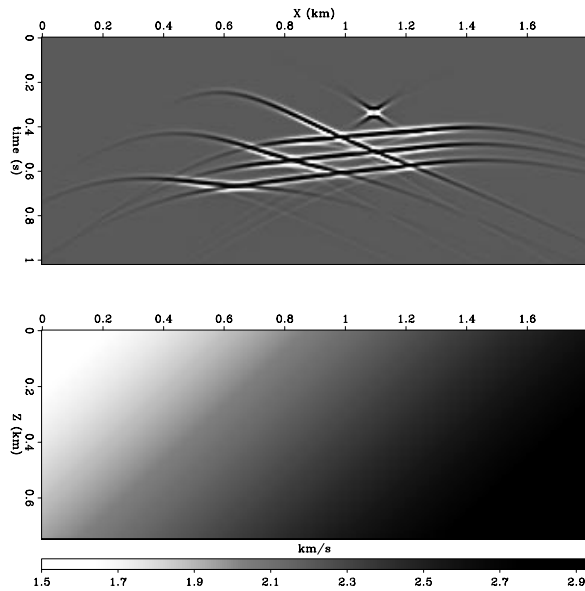# 3D wavefield extrapolation with helical boundary conditions

Figure 4: Cross-sections through zero-offset reflectivity model (top), and laterally variable velocity model (bottom).

For the migration, we used 20 reference velocities, and truncated filter coefficients when they became 10^3 times smaller than the leading value, with a maximum of 20 points. Filters contained $8-10$ coefficients for average frequencies.

Figure 4 shows the results of the migration. The three dipping beds are well imaged in cross-section, and in the depth-slice the effect of the velocity gradient is apparent from the slight azimuthal anisotropy of the impulse response.

CONCLUSIONS

Implicit extrapolations have the advantages over explicit methods, that they can be unconditionally stable, and shorter filters are required to achieve higher accuracy. Through the helical coordinate system, we have recast the 2-D deconvolution at the heart of implicit 3-D wavefield extrapolation, into a one-dimensional problem that can be solved efficiently by recursion. Lateral variations in velocity are handled by non-stationary deconvolution. While we have demonstrated our method by migrating a simple synthetic example with the $45°$ approximation, helical boundary conditions may be applied to the full range of implicit methods, making them viable for 3-D applications.

REFERENCES

Claerbout, J. F., 1976, Fundamentals of Geophysical Data Processing: Blackwell Scientific Publications.

Claerbout, J. F., 1985, Imaging the Earth's Interior: Blackwell Scientific Publications.

Claerbout, J. F., 1998, Invitation to the helical coordinate system: 68th Annual Internat. Mtg., Soc. Expl. Geophys., Expanded Abstracts (this edition).

Etgen, J. T., 1994, Stability of explicit depth extrapolation through laterally varying media: 64th Annual Internat. Mtg., Soc. Expl. Geophys., Expanded Abstracts, 1266–1269.

Gazdag, J., 1978, Wave equation migration with the phase-shift method: Geophysics, **43**, no. 7, 1342–1351.

Graves, R. W., and Clayton, R. W., 1990, Modeling acoustic waves with paraxial extrapolators: Geophysics, **55**, no. 3, 306–319.

Hale, 1990a, 3-D Depth migration via McClellan transformations: Geophysics, **56**, no. 11, 1778–1785.

Hale, 1990b, Stable explicit depth extrapolation of seismic wavefields: Geophysics, **56**, no. 11, 1770–1777.

Holberg, O., 1988, Towards optimum one-way wave propagation: Geophys. Prosp., **36**, no. 2, 99–114.

Iserles, A., 1996, A First Course in the Numerical Analysis of Differential Equations: Cambridge University Press.

Jenner, E., de Hoop, M., Larner, K., and van Stralen, M., 1997, Imaging using optimal rational approximation to the paraxial wave equation: 64th Annual Internat. Mtg., Soc. Expl. Geophys., Expanded Abstracts, 1750–1753.

Stoffa, P. L., Fokkema, J. T., de Luna Freire, R. M., and Kessinger, W. P., 1990, Split-step Fourier migration: Geophysics, **55**, no. 4, 410–421.

Wilson, G., 1969, Factorization of the covariance generating function of a pure moving average process: SIAM J. Numer. Anal., **6**, no. 1, 1–7.

Zhou, H., and McMechan, G. A., 1997, One-pass 3-D seismic extrapolation with the $45°$ wave-equation: Geophysics, **62**, no. 6, 1817–1824.
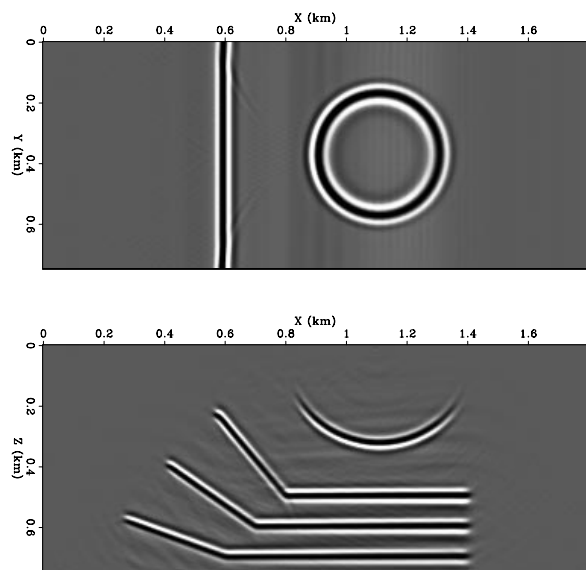
Figure 5: Results of 3-D implicit depth migration with the helical coordinate system: depth-slice at $Z = 0.25$ km (top), and cross-section at $Y = 0.375$ km (bottom).